Monte Carlo Studies of Dendrimer Macromolecules

Marc L. Mansfield* and Leonid I. Klushin†

Michigan Molecular Institute, 1910 West St. Andrews Road, Midland, Michigan 48640

Received March 23, 1993; Revised Manuscript Received May 13, 1993

ABSTRACT: Monte Carlo calculations on a set of diamond-lattice model dendrimers are reported. Equilibrium results through nine generations have been obtained, where the spacer in each generation is a seven-step walk on the lattice. We report data on radius of gyration, principal moments of inertia, chain extension, radial density profiles, and molecular scattering structure factors. We find that terminal groups are dispersed throughout the molecule, that spacers near the core are extended, and that the later generation dendrimers exhibit some hollowness.

1. Introduction

Dendrimer macromolecules are regularly branched polymers with a dendritic, treelike structure. Syntheses of a number of such macromolecules have now been reported,[1-6] with perhaps the most well-understood dendrimer being the polyamidoamide (PAMAM) molecule whose synthesis has been reported by Tomalia and coworkers.[1,2] These molecules are built from a central core trivalent nitrogen atom and are constructed from the following moiety:

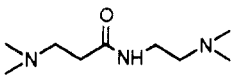

The molecules can be built up through a number of generations, with generation number designated as in Figure 1. Since the mass of the molecule is exponential in the generation number and grows much more rapidly than the available volume, the structure saturates at a given generation number, beyond which it is impossible to grow the molecule to completion.

A few theoretical or numerical studies of dendrimer molecules have now appeared. de Gennes and Hervet[7] presented a mean-field model which suffers from several deficiencies, namely: one, the assumption that all the segments belonging to a given generation lie in a concentric shell about the core, and an incorrect boundary condition applied to the last generation. These assumptions appear to be inconsistent with all later numerical studies of dendrimers, including the study reported here. Naylor et al. have published molecular mechanics and molecular dynamics studies of PAMAM dendrimers, using a detailed atomic-level force field.[8] These are quite interesting and illuminating studies, but since the molecular dynamics runs spanned times of only a few hundred picoseconds, it is questionable that the runs were long enough to remove any biases inherent in the initial structures, at least in the higher generations, since we estimate (see below) structural relaxation times for these molecules to be in the microsecond range. Furthermore, no mention is made of the technique by which the initial structures were generated, so it is impossible to determine the extent to which the initial structures depart from equilibrium. Lescanec and Muthukumar[9] have published a dendrimer model in which individual segments are modeled as strings of beads, strung together into molecules following a random growth process that they describe fully in their publication. Once again, the results are interesting and illuminating; however, the random growth process is not expected to rigorously sample the equilibrium ensemble and we have no way of knowing the degree of departure from equilibrium. We have also performed mean-field calculations on a model superficially similar to that of de Gennes and Hervet[7] but also patterned after the study of linear polymer melts made by Scheutjens and Fleer.[10] A report of that computation is in preparation.

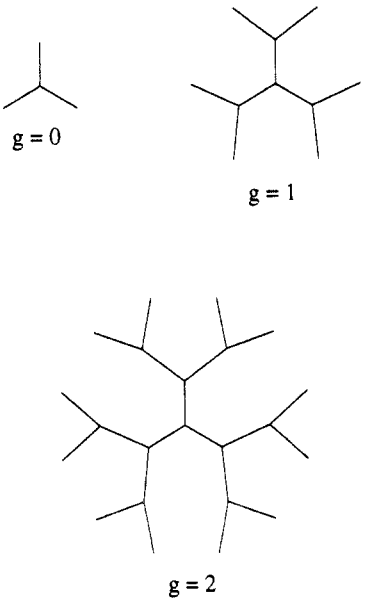

Figure 1. Schematic diagrams of dendrimer connectivity showing generation number.

In this paper, we report Monte Carlo calculations on a diamond lattice dendrimer model. Obviously, this model lacks the atomic detail of the Naylor et al.[8] study but has the advantage that we can be very confident that the results correspond to equilibrium. In the next section, we describe the model and the computational details and in subsequent sections we present results and discussion.

2. Description of the Model and of the Computational Procedures

We consider a model dendrimer, laid out on the diamond lattice. The dendrimer begins at the origin, with three individual strands or spacers, each spacer consisting of a seven-bond walk on the lattice. Then, each of these spacers has two daughter spacers, which are themselves seven-bond walks on the same lattice. All subsequent generations are built up in the same way, each spacer in one generation having two daughters in the next, and each spacer in each generation consisting of a seven-step walk. The total number of generations is denoted g. Then a $g=0$ model dendrimer contains three spacers, all connected at one

† Current address: Department of Physics, American University of Beirut, Beirut, Lebanon.

0024-9297/93/2226-4262$04.00/0

end to the origin, a $g=1$ dendrimer contains nine spacers, the three belonging to generation zero, and six daughters belonging to generation one, etc. We only consider completely self-avoiding dendrimers, i.e., only those for which no lattice site is ever visited twice. (We do, however, tolerate self-intersections in preliminary computer runs, but only as a computational convenience; see below for details.)

We employ a coordinate system in which valid steps on the lattice are any of the eight vectors:

$$a = (+1,+1,+1),\ a' = -a$$
$$b = (-1,-1,+1),\ b' = -b$$
$$c = (-1,+1,-1),\ c' = -c$$
$$d = (+1,-1,-1),\ d' = -d$$

Valid walks on the lattice are any sequences of these eight vectors that also satisfy two other conditions: First, primed and unprimed vectors must alternate in the walk, and second, immediate backsteps are disallowed by forbidding a′ to follow a, etc. The result is the standard, three-choice walk on the diamond lattice, since any one vector can only be followed by three others. Since there are eight choices for the first bond and three for successive bonds, there are $8(3^6) = 5832$ unique seven-step walks on the diamond lattice. Obviously, these exist in two separate parity classes, depending on whether the first bond in the sequence is primed or unprimed. These 5832 walks represent all possible states of every individual spacer in the dendrimer. Note that since each spacer contains an odd number of steps, the parity of the spacers alternates from one generation to the next, and since spacers in any given generation all have a given parity, then there are only $5832/2 = 2916$ possible states for any one spacer. Note also that we are employing units of length such that an individual bond has length $3^{1/2}$. All 5832 seven-step walks on the lattice are generated before-hand, and then stored in a look-up table in main memory during program execution. Obviously, a few of these 5832 spacer states are self-intersecting, but since the model is constructed to tolerate self-intersections in preliminary runs, all 5832 walks are included in the look-up table.

A given Monte Carlo step begins with the random selection of any spacer anywhere in the dendrimer. About half the time is an internal spacer, i.e., a spacer belonging to some generation other than the last, and therefore a spacer having daughters. Otherwise, it is a terminal or end spacer. If the selected spacer is an internal spacer, then an "internal wiggle" is attempted, while if it is an end spacer, an "end wiggle" is attempted.

An end wiggle is performed by replacing the state of the spacer in question with one of the 2916 possible states selected at random from the look-up table. The new state of the spacer is tentative pending a decision based on the change in the total number of self-intersections, as described below.

In performing an internal wiggle, the selected spacer and its two daughters are considered. Together these three spacers form a three-legged "spider". A successful internal wiggle leaves stationary the three feet, i.e., the three nodes at which the legs of the spider terminate, while permitting all other parts of the spider to move (see Figure 2). The central node of the spider is displaced by one of the following 12 vectors, selected at random: (±2, ±2, 0), (±2, 0, ±2), (0, ±2, ±2). The look-up table of spacer states is scanned for seven-step walks that are able to bridge the three new gaps between each foot of the spider and the new position of the central node of the spider. (To facilitate this step, the look-up table of spacer states is sorted and stored at the outset by end-to-end vector.) If no bridging walks can be found between any one foot and the central node, then the move is rejected. If more than one bridging walk can be found between any one foot and the central node, then a single one is selected randomly from among these. So, if successful, this procedure identifies a new, tentative configuration for the spacer and its two daughters. Ultimate selection of this tenative configuration depends on the change in total number of self-intersections, as described in the following paragraph.

Figure 2. An internal wiggle, one of two fundamental Monte Carlo moves, consists of moving one spacer and its two daughters (initial and final configurations represented by solid and dashed lines, respectively) while holding the rest of the molecule in place.

Obviously, we would like to study only self-avoiding dendrimers. One possible approach therefore is to begin from any given dendrimer configuration that is known to be self-avoiding and reject all wiggles that introduce self-intersections. However, we are unable to devise any particularly simple way of selecting an initial configuration that is known to be self-avoiding, except in the trivial case of small generation number. Our approach, therefore, has been to tolerate self-intersections at the outset and to reject all wiggles that increase the total number of these. Eventually, the total number of self-intersections falls to zero. Formally, this is equivalent to Metropolis Monte Carlo selection in which self-intersections are assigned a very large, finite energy, and elimination of self-intersections is performed as part of the equilibration phase of the Monte Carlo calculation. We obtain substantial savings in computation time by setting up an array to keep track of the number of segments occupying each lattice site. Then computation of the change in number of self-intersections is independent of molecular size, and overall computation times are nearly independent of the number of generations. On the IBM RS-6000, we were able to do 10^6 wiggles in about 5 to 6 cpu minutes. This technique was only applied at generations 8 and 9.

Obviously, important differences exist between this model and the PAMAM's or, for that matter, any other actual dendrimer molecule. This model includes no inherent difference between gauche and trans energy states and permits different spacers to approach one another to a distance of one bond length. Therefore, individual spacers in the Monte Carlo model are considerably more flexible and somewhat more slender than those in the PAMAM's. Likewise, all bonds have the same length, being $3^{1/2}$ in the units we employ. Furthermore, this model does not include hydrogen bonding, which may play an important role in determining structure, just as it does in the polypeptides. On the other hand, the model is expected to display those properties common to all dendrimers.

Three different techniques were employed to generate initial configurations for input to the Monte Carlo algorithm. The first technique, which creates what we have called "random" initial structures, assigns the internal states of all spacers in the molecule by random selection from the look-up table of spacer states. The second technique, generating so-called "augmented" structures, takes the structures of all spacers in generations through

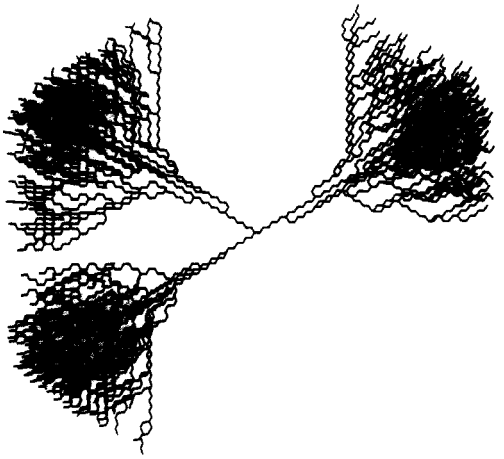

Figure 3. Baobab structures were created by applying a strong radial force on the terminal groups during the course of the computation. To be certain of equilibration, parallel runs were performed starting from a baobab structure on the one hand, and from a more compact structure on the other.

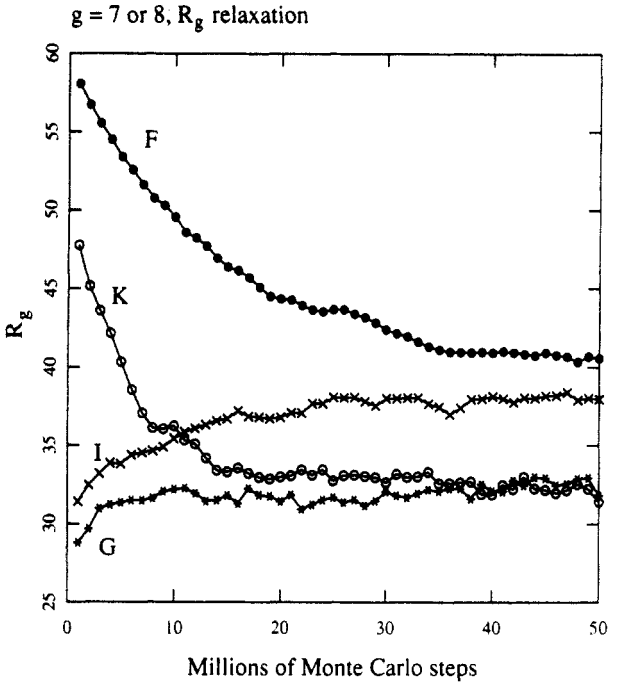

Figure 4. Equilibration, verified by convergence of R_g values from very dissimilar initial conditions, requires ca. 35 million wiggles at $g = 7$ and >50 million wiggles at $g = 8$.

$g-1$ from a well-equilibrated structure of $g-1$ generations and then adds the last generation by random selection from the look-up table. The third technique, providing "baobab" structures (so-called because of their resemblance to the baobab-infested planet of St. Exupéry's *Le Petit Prince*[11]), applies an artificial, strong radial force to each terminal group during an initial phase of the Monte Carlo calculation to produce a highly stretched structure. Then, this radial force is turned off and the structure permitted to relax. A typical baobab structure appears in Figure 3.

In the higher generations, we found that the Monte Carlo process relaxes so slowly that it is quite easy to mistake a steady drift toward equilibrium with a true equilibration. For example, Figure 4 displays radii of gyration, sampled at every million time steps for four separate runs, designated G, K, I, and F. Runs K and F were initiated from baobab structures, while runs G and I were initiated from augmented structures. Runs K and G were run at $g = 7$, while runs I and F were run at $g = 8$. Based solely on drift in R_g numbers, one might conclude that runs K and G have equilibrated after about 15 or 20 million cycles, but the actual equilibration time, based on convergence of the two runs, is obviously about 35 million cycles. At $g = 8$, additional calculations demonstrate that about 100 million cycles are necessary to achieve equilibrium. To be certain of equilibrium, we always performed parallel runs at the same generation number starting from both an augmented and a baobab structure. These two starting configurations are significantly different, one being relatively collapsed and the other highly stretched, and results from either calculation were not accepted until the two had converged to the same equilibrium. Convergence of the radius of gyration proves to be an acceptable test of equilibration, since all other sampled properties are also found to have converged.

Table I. Timing Statistics for Monte Carlo Calculations on IBM RS-6000

g	cycles required to equilibrate (millions)	estimated PAMAM relaxation time, μs
1	<1	
2	<1	
3	<1	
4	<1	
5	2	0.1
6	6	0.2
7	35	0.5
8	100	0.7
9	300	1.0

Following this initial equilibration phase of the Monte Carlo calculation, the Monte Carlo procedure continues through a sampling phase. At intervals of 1000 Monte Carlo cycles, the structure of the system is sampled for the following properties: (1) radius of gyration; (2) principle moments of inertia; (3) density as a function of distance from the core; (4) the fraction of trans bonds as a function of chemical distance (i.e., number of bonds) from the core. Then each of these properties is averaged over all samples taken. Also, after every million Monte Carlo cycles, the structure is recorded on hard disk, permitting additional properties to be sampled at that interval. We report below average values of the static structure factor obtained from samples taken every million Monte Carlo cycles.

Table I reports the number of Monte Carlo cycles required for equilibration, defined as the number of cycles required for both the baobab and augmented structures to converge to the same equilibrium. We also give in Table I an estimate of the relaxation time of actual PAMAM dendrimers. This approximation is based on the assumption that each Monte Carlo step in this model is equivalent to 10^{-11} s/M in the actual PAMAM dendrimers, where M is the number of spacers. A value of 10^{-11} s is taken as typical of the time scale for conformational transitions in the PAMAM's, this must be divided by the number of spacers since in nature conformational transitions occur simultaneously throughout the molecule. This is admittedly a very crude approximation, but at least indicates that structural relaxation times of around a microsecond are probably typical of PAMAM's in the range of seven to nine generations.

As mentioned above, the average conformational state of bonds in the dendrimer was also sampled. Each bond in the dendrimer is defined as either trans or nontrans. We sample the trans fraction, or the fraction of bonds that are trans, as a function of bond number, i.e., the chemical distance of the bond from the core of the dendrimer. We take the standard definition of a trans bond for those bonds not adjacent to the branch points of the dendrimer. When a bond is adjacent to a branch pont, we take the following definition for the trans state.

The bond in question (call it A) is attached at one end to a branch point and therefore to two bonds (call them B and C) and at the other end to a single bond (call it D). Then we can imagine a fifth bond (called E) attached at the branch point in such a way as to complete the tetrahedral tetrad at the branch point. (If the branch point in question were a nitrogen atom, then bond E would give the orientation of the lone pair of electrons belonging to the nitrogen atom.) Then bond A is assumed to be a trans bond if the three bonds EAD have the standard trans arrangement.

Two different approaches were attempted to compute single molecule scattering structure factors. The structure factor for a single molecular configuration, including orientational averaging, is defined as

$$S(q) = \frac{1}{4\pi N^2} \sum_{j=1}^{N} \sum_{k=1}^{N} \int_0^{2\pi} d\varphi \int_0^{\pi} \sin\theta \, d\theta \exp[i\mathbf{q}\cdot\mathbf{r}_{jk}] \quad (1)$$

where the vectors $\mathbf{q}$ and $\mathbf{r}_{jk}$ are

$$\mathbf{q} = q(\sin\theta\cos\varphi, \sin\theta\sin\varphi, \cos\theta)$$
$$\mathbf{r}_{jk} = \mathbf{r}_j - \mathbf{r}_k$$

and where $\mathbf{r}_j$ and $\mathbf{r}_k$ are the vector positions of the jth a nd kth scattering centers, respectively, and N is the total number of scattering centers. For these computations, we place a scattering center at each occupied lattice site. If the average over orientations is performed before the double sum over scattering centers, then eq 1 can be written

$$S(q) = \frac{1}{N^2} \sum_{j=1}^{N} \sum_{k=1}^{N} \frac{\sin(qr_{jk})}{qr_{jk}} \quad (2)$$

On the other hand, if the double sum over scattering centers is performed before the orientational average, then the former sum is separable

$$S(q) = \frac{1}{4\pi N^2} \int_0^{2\pi} d\varphi \int_0^{\pi} \sin\theta \, d\theta \left|\sum_{j=1}^{N} \exp[iq\cdot r_j]\right|^2 \quad (3)$$

Obviously, the time to compute $S(q)$ by eqs 2 and 3 is proportional to N^2 and N, respectively, so eq 3 is the method of choice for large N. However, eq 3 has the disadvantage that the average over orientations must be done numerically, so that eq 2 is faster for small N. We did the orientational average of eq 3 at intervals of 5° in both θ and φ and found eq 3 to be slower than eq 2 for all dendrimers through six generations and only slightly slower at seven generations. Therefore the structure factors reported below were obtained using eq 2. The computation of $S(q)$ is costly, except in the early generations, and so $S(q)$ was evaluated only after every million Monte Carlo steps for dendrimers with g between 3 and 7, every thousand steps when $g = 1$ or 2, and not at all for $g = 8$ or 9. Since typical sampling runs had durations of on the order of 10 million cycles, typical sample sizes for the $S(q)$ computation were about 10 or 20 when $g \geq 3$. Obviously, therefore, the $S(q)$ results given below for $g \geq 3$ are rather tentative. However, we generally give $S(q)$ results for two or more independent series of runs, and, find the reproducibility to be moderately good over the q ranges sampled. The $g = 1$ and $g = 2$ calculations with sampling every 10^3 samples were highly reproducible, the $g = 3, 4, \ldots, 7$ with sampling every 10^6 samples were somewhat less so.

3. Results

Table II summarizes all the computer runs from which data are reported in this paper. It reports (1) the number of generations, (2) the way in which an initial structure was provided for the run, (3) the number of Monte Carlo cycles performed in both equilibration and sampling phases, and (4) the root mean square radius of gyration obtained by averaging over the sampling phase of the run. Figure 5 displays perspective projections of typical structures. The root mean square radius of gyration as a function of generation number appears in Figure 6. The ratios of the average moments of inertia appear in Figure 7. These are sorted in ascending order $M_1 < M_2 < M_3$ and displayed as the ratios M_1/M_2 and M_3/M_2. As the generation number increases, these two ratios approach unity, which indicates that the dendrimers are becoming progressively more spherical, a trend first observed by Naylor et al.[8] in their simulations.

Radial Densities. Figure 8 displays radial densities, averaged over all dendrimers sampled at each generation

Table II

g	initial structure[a]	R_g	equilibrium steps (millions)	sampling steps (millions)
1	B	7.58	5	5
1	R	7.59	5	4
1	B	7.59	1	5
1	R	7.58	1	5
1	R	N.A.[b]	1	5
2	B	10.80	1	9
2	A	10.84	1	9
2	R	10.81	1	9
2	R	N.A.[b]	1	5
3	A	14.14	1.2	10
4	R	17.64	6	11
4	B	17.78	6	11
5	B	22.11	3	11
5	A	22.17	3	11
6	A	26.43	26	23
7	A	32.43	34	16
7	B	32.38	34	16
8	A	38.53	100	400
8	B	38.57	100	380
9	A	45.29	300	100
9	B	45.51	300	100

[a] Initial structures were either A (augmented), B (baobab), or R (totally random). See text for details. [b] Gyration radii not calculated in these runs. They were used to produce structure factors only.

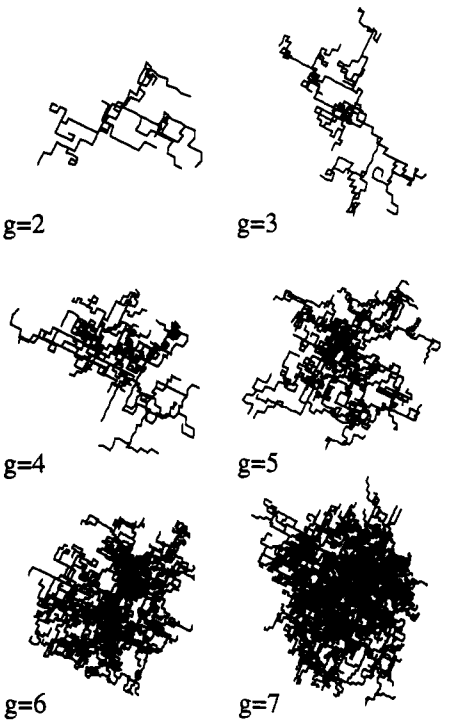

Figure 5. Projections of typical dendrimer structures.

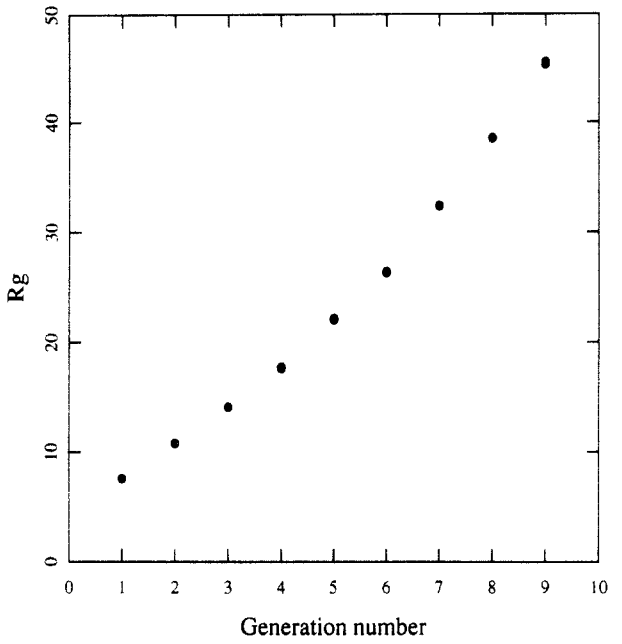

Figure 6. Radius of gyration as a function of generation number, g.

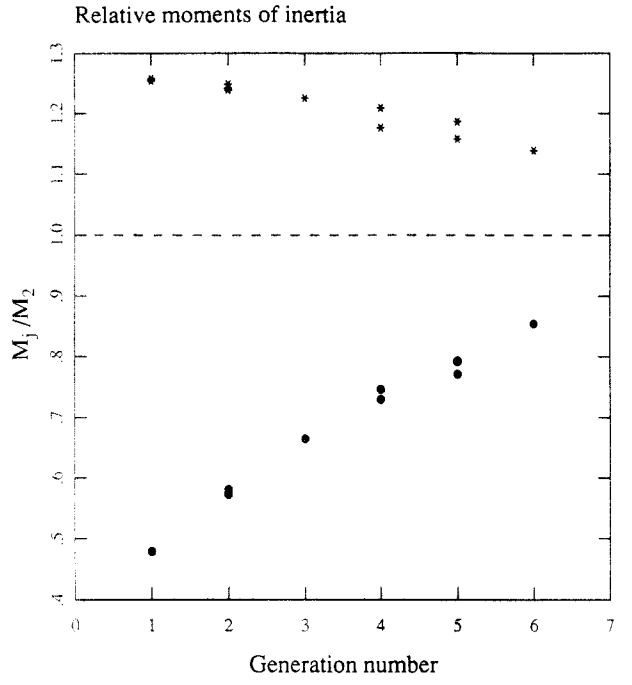

Figure 7. Relative values of the three principal moments of inertia, sorted in ascending order $M_1 < M_2 < M_3$.

number. These give the number density of segments in concentric shells, each of thickness 2, about the origin. Typically, radial densities in the lower-generation dendrimers are monotone decreasing, while in the higher-generation dendrimers they pass through a relative minimum at about shell 5 (or at a radius of about 8 or 10) before first increasing and then finally decreasing again. (The structure observed in shells 2 and 3 is assumed to be an artifact of the lattice and not expected to be observed in continuum models.)

Figure 9 gives radial densities at $g = 7$ and displays the contribution to the density from the last generation. It is obvious that segments belonging to the last generation are dispersed completely throughout the molecule.

Trans Fractions, Degree of Extension of Individual Spacers. As explained above, we accumulated data on the trans fraction as a function of chemical distance, or

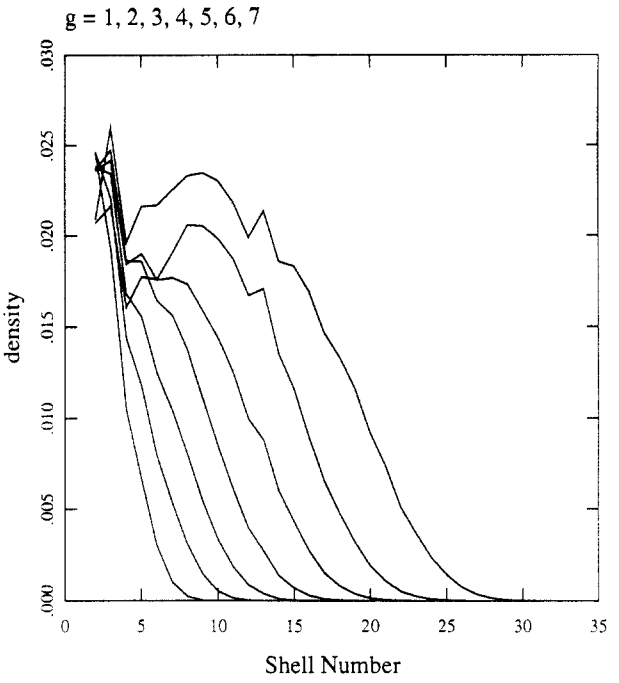

Figure 8. Number densities of dendrimer segments found in concentric shells centered at the dendrimer core.

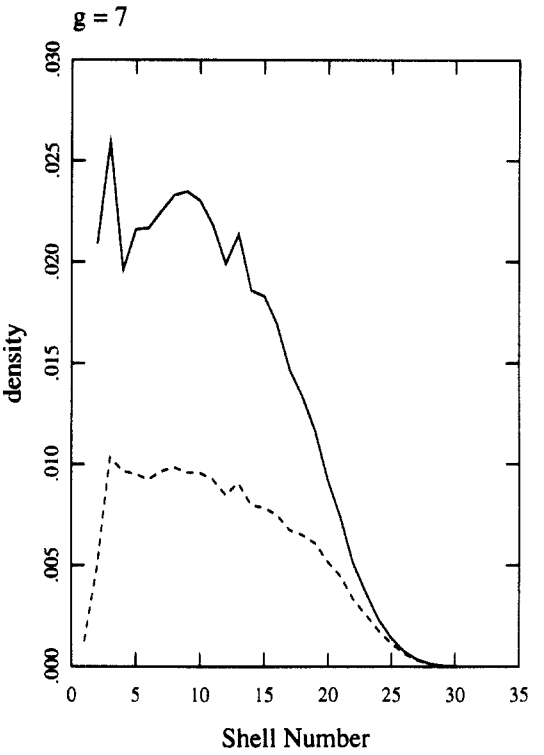

Figure 9. Number density of dendrimer segments found in concentric shells for $g = 6$: solid curve, all segments; dashed curve, contribution from terminal spacers.

bond number, from the core of the molecule in order to determine the degree to which individual spacers become extended. A few typical results are shown in Figures 10–12, for dendrimers of $g = 1$, 5, and 7, respectively. Solid lines are drawn through every seventh data point, and therefore connect data from equivalent bonds in one generation to the next. Even in the $g = 1$ dendrimer the generation zero spacers are somewhat stretched, with trans fractions near 0.5. As we go to larger dendrimers, the inner generations become progressively more extended, until at $g = 7$ the innermost bonds have trans fractions approaching either 0 or 1. (Given our specific definition of trans fraction for bonds adjoining a branch point, the

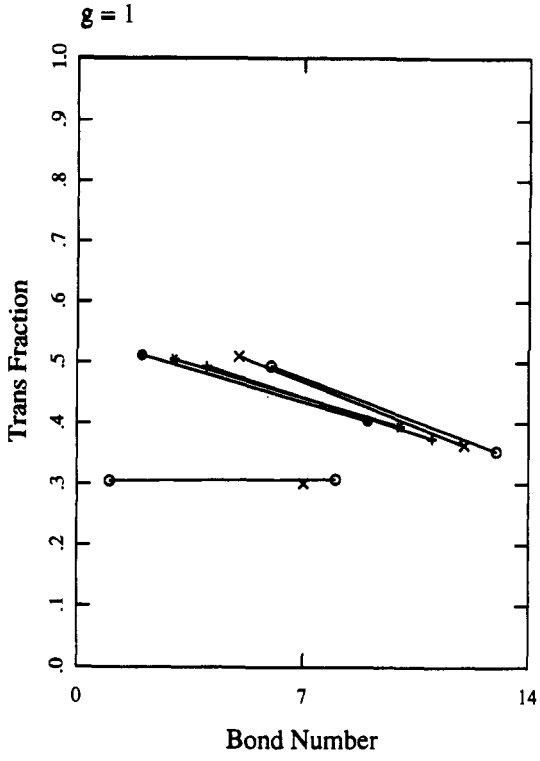

Figure 10. Trans fraction of a function of chemical distance from the core for $g = 1$ dendrimers.

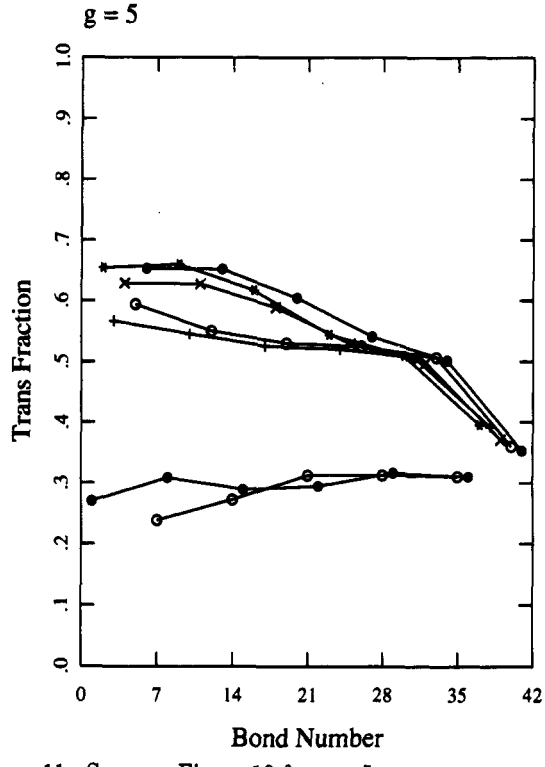

Figure 11. Same as Figure 10 for $g = 5$.

trans fraction of such bonds is expected to decrease with chain stretching.) In contrast, in every case, the outer tier of spacers is almost completely relaxed with trans fractions always near $^1/_3$. These data indicate that the earlier generations are always more extended than the outer ones, that the last generation is always almost completely unstretched, and that the inner generation is almost completely extended in the $g = 7$ dendrimer.

Scattering Structure Factors. Single molecule scattering structure factors are displayed in Kratky representation in Figure 13. For purposes of comparison, the Kratky plot for a hard sphere is also displayed. As

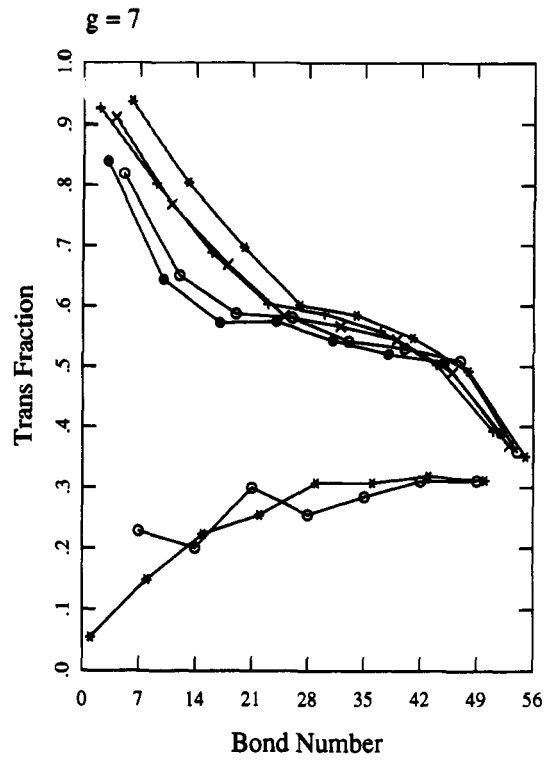

Figure 12. Same as Figure 10 for $g = 7$.

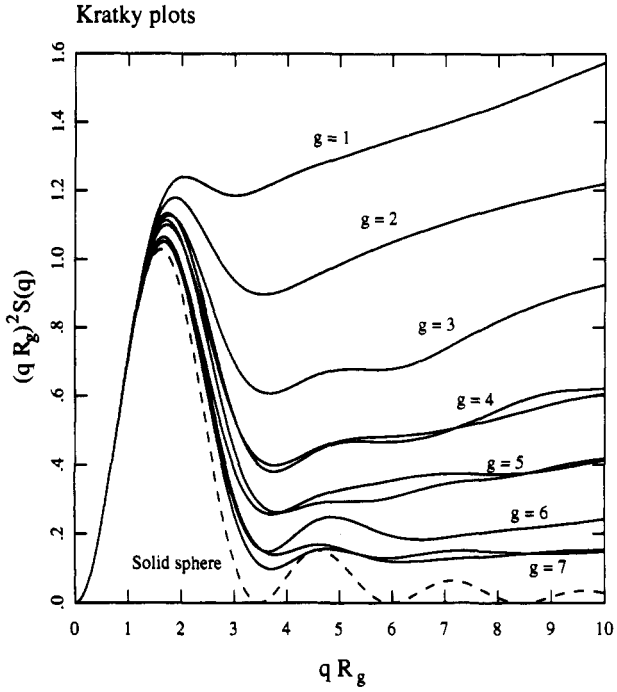

Figure 13. Single particle scattering factors in Kratky representation for the dendrimers of indicated g value. The dashed curve gives the scattering factor for a solid sphere.

described above, the sample size for this computation is extremely small except when $g = 1$ or 2, nevertheless, fairly good reproducibility is obtained between different parallel runs at the same value of g. Therefore, these results are probably fairly accurate.

There is not yet available a great deal of neutron scattering data on dendrimers. Bauer et al.[12] have reported experimental single particle structure factors for a $g = 7$ PAMAM dendrimer with data in the range $0 < qR_g < 3.4$. Some measurements in the range $0 < qR_g < 9$ on $g = 9$ PAMAM dendrimers have also been reported to us.[13] These preliminary results appear to agree rather well with the higher generation structure factors appearing in Figure

13, including the existence of a secondary Kratky peak in the region $4 < qR_g < 8$. Note also that the dendrimer curves appear to approach the curve of a hard sphere as the molecule becomes larger.

4. Conclusions

These calculations illuminate a number of properties of dendrimer macromolecules. Even though this model differs in several fundamental ways from actual dendrimer molecules, it very likely gives qualitative agreement with their properties. The important properties exhibited by this model include the following.

1. Not all the end groups lie near the exterior of the molecule. Rather, they are dispersed throughout the molecule and may even be found in close proximity to the central core. About half the mass of the molecule is found in the terminal spacers, and it follows that all regions, including the exterior surface, are saturated with end groups.

2. Relaxation times for this Monte Carlo procedure are a strong function of generation number. This probably reflects a similar property of the dynamics of actual dendrimers.

3. The spacers belonging to the early generations are extended, with the amount of extension increasing with the total number of generations. This is an obvious consequence of molecular crowding; excluded volume forces exert strong tensions on spacers near the core of the molecule. On the other hand, terminal spacers are always relaxed.

4. There is a range of generation numbers for which some hollowness is indicated, seen, for example, in Figure 8 as regions of relative minimum in density vs radial distance. The central spacers become well-extended to maximize the total volume available to the molecule. Later spacers are backfolded, but apparently the backfolding is inadequate to completely refill the voids created by the extended central spacers. It is not known if this hollowness will continue to be observed in larger dendrimers.

5. Neutron scattering patterns predicted for this model are in good agreement with the limited experimental data now available, showing one major Kratky peak in the range $0 < qR_g < 3.5$ and a minor Kratky peak in the range $3.5 < qR_g < 6$.

Acknowledgment. The authors are grateful for a number of useful discussions with Drs. D. A. Tomalia and D. M. Hedstrand and for their encouragement of this work. We are also grateful to Professor R. M. Briber and Dr. B. J. Bauer for providing us with the neutron scattering data appearing in refs 12 and 13. Partial support for this research was provided by the National Science Foundation, Grant DMR-8822934.

References and Notes

(1) Tomalia, D. A.; Baker, H.; Dewald, J.; Hall, M.; Kallos, G.; Martin, S.; Roeck, J.; Ryder, J.; Smith, P. *Polym. J.* **1985**, *17*, 117.
(2) Tomalia, D. A.; Hedstrand, D. M.; Wilson, L. R. *Encyclopedia of Polymer Science and Engineering*, 2nd ed.; Wiley: New York, 1990; Index vol., pp 46–92.
(3) Tomalia, D. A.; Naylor, A. M.; Goddard, W. A., III *Angew. Chem., Int. Ed. Engl.* **1990**, *29*, 138.
(4) Hawker, C. J.; Fréchet, J. M. J. *Macromolecules* **1990**, *23*, 4726.
(5) Morikawa, A.; Kakimoto, M.; Imai, Y. *Macromolecules* **1991**, *24*, 3469.
(6) Newkome, G. R.; Lin, X. *Macromolecules* **1991**, *24*, 1443.
(7) de Gennes, P. G.; Hervet, H. *J. Phys. (Paris)* **1983**, *44*, L351.
(8) Naylor, A. M.; Goddard, W. A., III; Kiefer, G. E.; Tomalia, D. A. *J. Am. Chem. Soc.* **1989**, *111*, 2339.
(9) Lescanec, R. L.; Muthukumar, M. *Macromolecules* **1990**, *23*, 2280.
(10) Scheutjens, J. M. H. M.; Fleer, G. J. *Macromolecules* **1985**, *18*, 1882.
(11) St.-Exupéry, A. *Le Petit Prince*; Editions Gallimard: Paris, 1946; p 25.
(12) Bauer, B. J.; Briber, R. M.; Hammouda, B.; Tomalia, D. A. Preprint.
(13) Bauer, B. J. Private communication to D. A. Tomalia.